Rare Metal Materials and Engineering
Volume 47, Issue 4, April 2018
Online English edition of the Chinese language journal

Available online at www.sciencedirect.com
ScienceDirect

Cite this article as: Rare Metal Materials and Engineering, 2018, 47(4): 1069-1074.

ARTICLE

Effect of Ti_3AlC_2 Content on Mechanical Properties of Ti_3AlC_2/ZA27 Composites

Li Haiyan, Zhou Yang, Cui Ao, Li Shibo, Huang Zhenying, Zhai Hongxiang

Beijing Jiaotong University, Beijing 100044, China

Abstract: ZA27 alloy-based composites reinforced by 10~40 vol% Ti_3AlC_2 particles were prepared by pressureless sintering mechanically alloyed powders at 870 °C for 2.5 h. The effects of Ti_3AlC_2 content on hardness, density, stretching and bending performance were studied. The results demonstrate that a well bonded interface could be obtained by weak reaction occurring at the interface between Ti_3AlC_2 and ZA27 alloy during sintering process, which is beneficial to the mechanical properties of the Ti_3AlC_2/ZA27 composites. An increase in Ti_3AlC_2 content (up to 30 vol%) leads to enhanced hardness and mechanical strength of the composites due to dispersion strengthening of nano-sized Ti_3AlC_2 particle. However, with an increase in Ti_3AlC_2 content to 40 vol%, the hardness and strength decrease because of the growing number of pores. Compared the four composites with different Ti_3AlC_2 contents, the 30Ti_3AlC_2/ZA27 composite possesses the best properties of 310 MPa for tensile strength, 528 MPa for bending strength and 1236 MPa for Vickers hardness. Besides the good interfacial bonding, the improved mechanical properties of the Ti_3AlC_2/ZA27 composites are also attributed to the fine-grained microstructure and well dispersed reinforcements.

Key words: Ti_3AlC_2/ZA27 composites; interfaces; mechanical properties

Since the ZA27 alloy (Zn-27wt% Al) was reported to be one of the top three in terms of high-performance, high aluminium zinc casting alloys, it has been widely used in low speed, high load bearings, and bushing applications[1]. However, a main problem, which directly relates to its applications, is the poor mechanical properties of the alloy at elevated temperatures above 100 °C[2]. Ceramic phase reinforcement appears to be an effective way to improve the high-temperature properties of ZA-alloys. Researches on ZA-alloy matrix composites reinforced with different ceramic particles showed that the composites exhibit high elastic modulus[3,4], wear strength[5,6], and corrosion resistance[7] compared with the parent matrix alloy. So preparation of zinc-base composites with good comprehensive performance has gained considerable attention.

In recent years, many works were focused on $M_{n+1}AX_n$ ceramics (M is a transition metal, A is a group IIIA to VIA element and X is C or N, n = 1~3). It is now well known that, the A atom in *MAX* phases is weakly bonded to M, whereas the covalent *M-X* bonds are much stronger. Such a specificity endows *MAX* phases not only ceramic properties, but also metallic properties. In addition, weakly bonded A atom layers may be out-diffused from the *MAX* phase under certain conditions[8-15]. As one of the typical representative of the *MAX* family, Ti_3AlC_2 phase has caught our eyes due to its good combination of specially mechanical, electrical, thermal, and chemical properties[16]. Considering the Al atom broken away from Ti_3AlC_2, a strong chemical affinity is expected between Ti_3AlC_2 and molten ZA27, where Al is one of the alloying elements. Besides, compared with other reinforcements of Zn-matrix composites (ZMC), as shown in Table 1[17-19], the thermal expansion coefficient of Ti_3AlC_2 is closer to that of ZA27 than the others. Hence, Ti_3AlC_2 has a potential to be an ideal enhancement phase of ZA27 alloy.

Main purpose of this work is to study the effect of the volume fraction of Ti_3AlC_2 reinforcement on the mechanical properties of Ti_3AlC_2/ZA27 composites prepared by pressure-

Received date: April 20, 2017
Foundation item: The Fundamental Research Funds for the Central Universities (2015YJS143)
Corresponding author: Zhou Yang, Ph. D., Professor, School of Mechanical & Electronic Control Engineering, Beijing Jiaotong University, Beijing 100044, P. R. China, Tel: 0086-10-51685554, E-mail: yzhou@bjtu.edu.cn

Table 1 Thermal expansion coefficients of ZA27 alloy and reinforcement phases applied in ZMC ($\times 10^{-6}$)

ZA27	Ti_3AlC_2	Graphite	Si_3N_4	SiC	TiC	Al_2O_3	Si
25.9	9.0	2.57	2.11	5.4	6.52	6.8	3.0

less sintering a mixture of mechanically alloyed Ti_3AlC_2 and ZA27 powders. X-ray diffraction, scanning electron microscopy and transmission electron microscopy were used to characterize the phase composition and microstructure of the Ti_3AlC_2/ZA27 composites.

1 Experiment

A commercial ZA27 powder (particle size <200 μm, Hunan Luxixian Antai New Materials Company, China) and the home-made Ti_3AlC_2 powder (purity 98%, average particle size 6.8 μm)[20] were used as the starting materials. Here, the Ti_3AlC_2 powder was synthesized by pressureless sintering a mixture of Ti:Al:1.8TiC:0.2Sn (molar ratio) at 1450 °C with a holding time of 10 min in Ar atmosphere. The heating rate was 30 °C/min. The volume ratio of Ti_3AlC_2 to ZA27 was selected as 1:9, 2:8, 3:7 and 4:6. The two powders were mixed using a planetary mill (QM-3SP4) for 3 h in a steel containers under vacuum with rotational speed of 300 r/min and ball-to-powder mass ratio of 10:1. The mixed powders were firstly compacted into a cylindrical green body with 50 mm in diameter and ~8 mm in thickness, and then the body was isostatically cold-pressed (KJYc 200-600/300) with 220 MPa for 2 min. All the four Ti_3AlC_2/ZA27 composites were pressurelessly sintered at 870 °C for 2.5 h in Ar atmosphere with a heating rate of 30 °C/min.

Phase composition of the four samples were identified by X-ray diffraction (D8 ADVANCE A25, Bruker, Germany). The density of the composites was tested by Archimedes method in distilled water using four parallel specimens. The theoretical density of the testing composites was determined by the equation:

$$\rho = \rho_1 \times f_1 + \rho_2 \times (1 - f_1) \quad (1)$$

where ρ_1 and ρ_2 are the theoretical density of the Ti_3AlC_2 and ZA27 alloy (5.0 g/cm^3), respectively, and f_1 is the volume fraction of Ti_3AlC_2 particle.

Both the tensile and bending tests were conducted at a loading speed of 0.3 mm/min at room temperature, and the average strength values of four specimens were obtained for each composite. Dimensions of the tensile specimen are shown in Ref. [21] with a thickness of 2 mm. The flexural strength was measured with the specimens of 3 mm×4 mm×36 mm using a three-point bending device (SUNS UMTM4204, China) with a span size of 30 mm. Hardness of all samples was measured by a Vickers hardness tester (HVS-1000 Z, China) using a static load of 20 N and a dwell time of 15 s. The fracture surfaces and polished surfaces of specimens were observed using a scanning electron microscope (JSM 6700F, JEOL, TOKYO, JAPAN). Microstructure of the Ti_3AlC_2/ZA27 composites was characterized by a high resolution transmission electron microscope (TECNAI F20, FEI, USA) equipped with an energy dispersive X-ray analysis (EDS) system.

2 Results and Discussion

2.1 Morphology of the mechanically alloyed powder

Fig.1 provides the morphologies of raw ZA27 powder and as-mechanically alloyed (MAed) mixtures of Ti_3AlC_2 and ZA27 powder with a volume ratio of 3:7. It can be seen clearly from Fig.1b that the mixture powders agglomerate together to form larger clusters with different sizes owing to cold welding effect. Careful observation of an agglomerate reveals that each cluster consists of much fine particles with size of about 5 μm (shown in Fig.1c). Compared with the raw ZA27 powder exhibited in Fig.1a, mechanical alloying technology decreases the particle sizes from ~20 μm to 5 μm.

2.2 XRD analysis of the Ti_3AlC_2/ZA27 composites

XRD patterns of the four samples are shown in Fig.2. Besides the main phases of Zn rich phase, Al rich phase and Ti_3AlC_2, two new phases of $Al_{0.64}Ti_{0.36}$ and TiC were detected in the composites. However, the contents of the two new phases are minor according to the result of quantitative analysis using a Jade software. It can be deduced that a small amount of Ti_3AlC_2 decomposed into TiC, Al and $Al_{0.64}Ti_{0.36}$ at the sintering temperature of 870 °C under an effect of matrix alloy. The reaction could be expressed as follows[21]:

$$Ti_3AlC_2 \xrightarrow{ZA27} Al_{0.64}Ti_{0.36} + TiC + Al \quad (2)$$

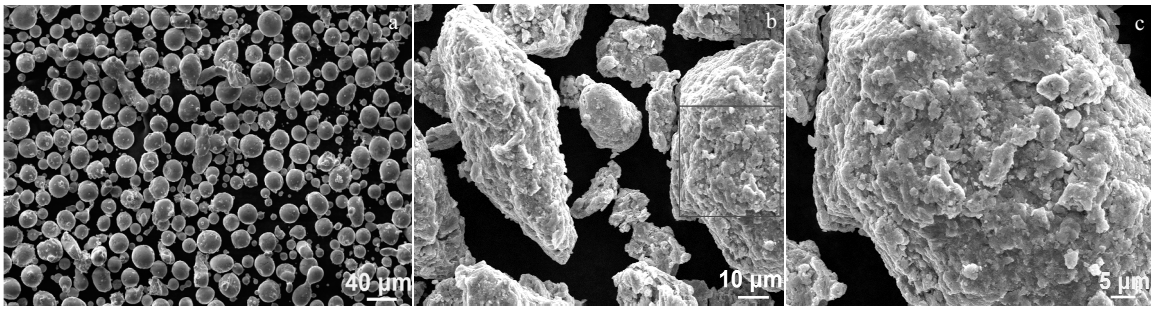

Fig.1 SEM micrographs of raw ZA27 powders (a) and as-MAed mixture of Ti_3AlC_2 and ZA27 powders (b, c)

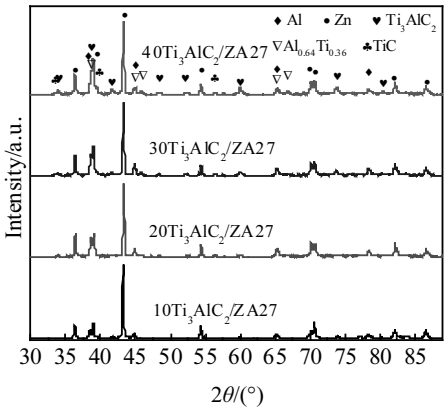

Fig.2 XRD patterns of the Ti_3AlC_2/ZA27 composites

Here, liquid ZA27 plays a role as catalyst because it could provide an easy diffusion path for Al atom. Generally, Ti_3AlC_2 is stable until 1400 °C in vacuum without any liquid metal[22]. Decomposition of Ti_3AlC_2, induced by the de-intercalation of Al atoms from Ti_3AlC_2, is promoted by the appearance of liquid ZA27, and leads to the formation of TiC[23].

2.3 Relative density analysis of the Ti_3AlC_2/ZA27 composites

Table 2 shows some fundamental physical and mechanical properties of the Ti_3AlC_2/ZA27 composites. Relative density (RD), which represents the defect level of materials, has a great impact on the mechanical properties of the composites. Relationship between RD of the composites and content of Ti_3AlC_2 reinforcement is shown in Fig.3. It is clear that relative densities of the Ti_3AlC_2/ZA27 composites show a monotonic decrease with an increase in Ti_3AlC_2 addition, from 93.1% for 10 vol% Ti_3AlC_2 to 87.7% for 40 vol% Ti_3AlC_2. It needs to be noted that the theoretical density of TiC (4.25 g/cm^3) and $Al_{0.64}Ti_{0.36}$ (3.55 g/cm^3) are similar to the density of Ti_3AlC_2 (4.25 g/cm^3). Moreover, the content of the new phases is very low because of the weak interface reaction, so we ignores the change of composite theoretical density after reaction

In accord with the result of RD, morphologies of tensile fracture surface for the Ti_3AlC_2/ZA27 composites demonstrate that the number of pores increase with an increase in Ti_3AlC_2 content, as shown in Fig.3. As a whole, the fracture surfaces of

Table 2 Experimental data of Ti_3AlC_2/ZA27 composites

Sample	RD/%	UTS/MPa	UBS/MPa	Elongation/%	Hardness/MPa
10Ti_3AlC_2/ZA27	93.1±0.4	190±11	369±16	0.78	999±78
20Ti_3AlC_2/ZA27	91.5±0.3	261±13	470±14	0.92	1178±100
30Ti_3AlC_2/ZA27	90.9±0.5	310±4	528±6	1.42	1236±72
40Ti_3AlC_2/ZA27	87.7±0.3	239±5	399±3	0.94	1224±72

*UTS: ultimate tensile strength; UBS: ultimate bending (or flexural) strength

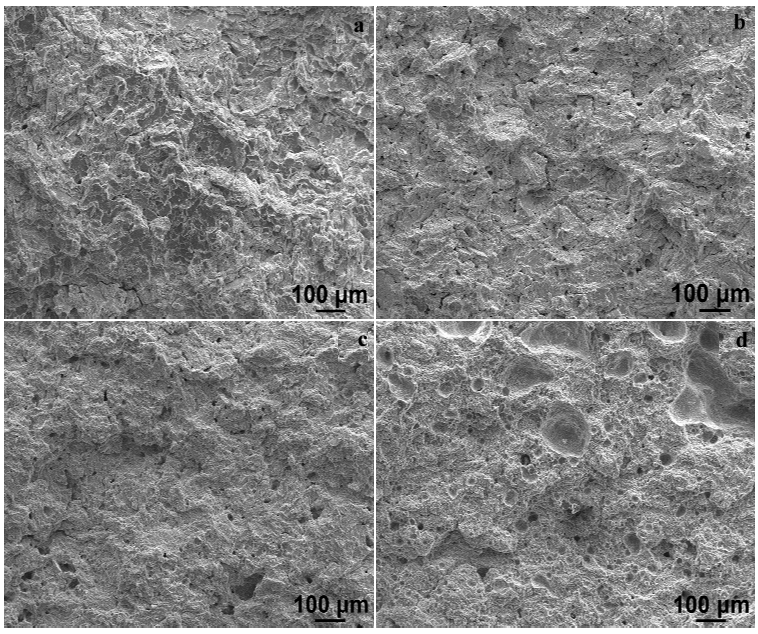

Fig.3 Fractographs of tensile fracture surfaces of the Ti_3AlC_2/ZA27 composites: (a) 10Ti_3AlC_2/ZA27, (b) 20Ti_3AlC_2/ZA27, (c) 30Ti_3AlC_2/ZA27, and (d) 40Ti_3AlC_2/ZA27

all composites are smooth, and no obvious dimples can be found. So a brittle fracture feature of the Ti_3AlC_2/ZA27 composites is deduced.

2.4 Strength analysis of the Ti_3AlC_2/ZA27 composites

Fig.4a shows the tensile stress-strain curves of the testing Ti_3AlC_2/ZA27 composites containing various Ti_3AlC_2 contents. Generally, all the four composites have low ductility as shown in this diagram. Among them, the 30Ti_3AlC_2/ZA27 has the highest elongation rate of 1.45%, and the 10Ti_3AlC_2/ZA27 has the minimum value of 0.78%. Fig.4b exhibits the average tensile and flexural properties of the Ti_3AlC_2/ZA27 composites. Within Ti_3AlC_2 volume fraction limits of 10~30 vol%, both the tensile strength and flexural strength of the composites are gradually improved with an increase in Ti_3AlC_2 content. But the two kinds of strength drop as the Ti_3AlC_2 volume fraction reaches to 40 vol%. The 30Ti_3AlC_2/ZA27 composite possesses the highest tensile strength of 310 MPa, which is 53% higher than 203 MPa for ZA27 matrix[24], and the highest flexural strength of 528 MPa, which is 55% higher than 340 MPa for Ti_3AlC_2 [25]. While the 10Ti_3AlC_2/ZA27 has the lowest mechanical strength among the four samples. Therefore, the content of Ti_3AlC_2 plays a key role in mechanical properties of the Ti_3AlC_2/ZA27 composites. On the premise of good interface bonding and uniform distribution, the more Ti_3AlC_2 particles are added, the higher strength are achieved in the Ti_3AlC_2/ZA27 composites. That means the strengthening effect of the Ti_3AlC_2 reinforcement is outstanding. However, pores are also increased in the composites with an increase in content of Ti_3AlC_2. Particularly, when Ti_3AlC_2 volume fraction reaches to 40 vol%, some macro pores are observed in 40Ti_3AlC_2/ZA27 (Fig.3d), and a brittle rupture occurs under a lower stress level for the 40Ti_3AlC_2/ZA27 composite.

Fig.5a displays a representative TEM image of the 30Ti_3AlC_2/ZA27 composite. It can be seen that Ti_3AlC_2 particle (marked by white solid arrows) with sizes of 40~60 nm are uniformly distributed in ZA27 matrix formed by Zn rich phase (the black area) and Al rich phase (the white area). Dispersion strengthening of the nano-sized Ti_3AlC_2 particles, which is attributed to mechanical alloying, is another reason for the high mechanical properties of the Ti_3AlC_2/ZA27 composites. A high-resolution TEM (HRTEM) image of the boundary between Ti_3AlC_2 and Al rich phase, as shown in Fig.5b, exhibits a well bonded interfaces between reinforcement and matrix without any defects, which endow the composites with enhanced mechanical properties. Although some reaction happens according to the result of XRD, there is no obvious interfacial reaction zone on the boundary. That means the reaction is weak, and not every Ti_3AlC_2 particle is involved in

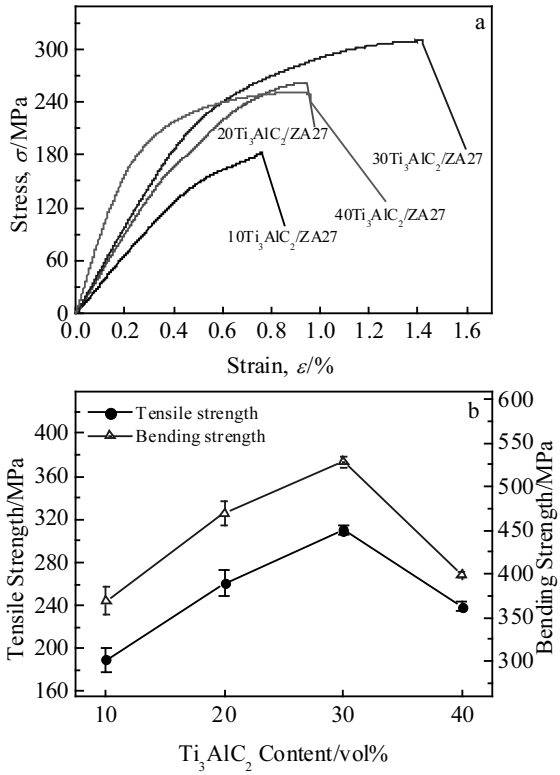

Fig.4 Tensile stress-strain curves of the Ti_3AlC_2/ZA27 composites (a) and ultimate tensile strength and bending strength of the Ti_3AlC_2/ZA27 samples at room temperature (b)

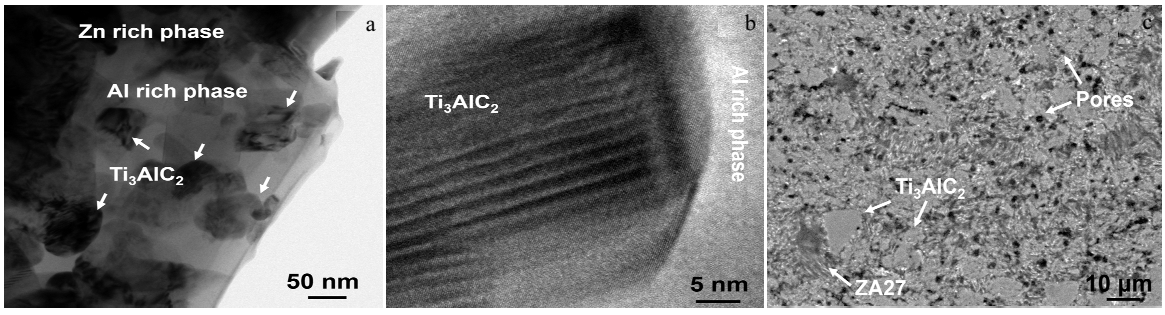

Fig.5 Typical TEM microstructure of 30Ti_3AlC_2/ZA27 composite (a), HRTEM image of the interface between Ti_3AlC_2 and matrix (b), and BSE image of polished surface of 30Ti_3AlC_2/ZA27 composite (c)

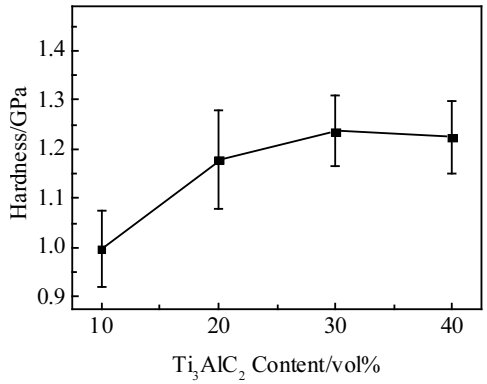

Fig.6 Effect of Ti_3AlC_2 content on hardness of the Ti_3AlC_2/ZA27 composites

decomposition reaction. The high mechanical strength of the composite could also be attributed to the homogeneous dispersion of the Ti_3AlC_2 particle, as shown in Fig.5c. In spite of some black pores on the sample surface, there are no large flaws in the composites, which indicate a weak effect of the pores on the mechanical properties of the composites.

2.5 Hardness analysis of the Ti_3AlC_2/ZA27 composites

It is different from the trend of RD curve that the hardness curve of the composites, as shown in Fig.6, changes in the opposite direction as the content of Ti_3AlC_2 increases. Since the hardness of Ti_3AlC_2 (2.0~5.0 GPa[26]) is much higher than that of ZA27 (1215 MPa)[27], which is approximately equal to 1192 MPa), an increase in hardness for the composite with more harder particles is expected. However, the maximum hardness of 1236 MPa is reached for the Ti_3AlC_2/ZA27 composites with 30 vol% reinforcement. A slight decrease in hardness for the 40Ti_3AlC_2/ZA27 composite is caused by the growing number of defects which collapses under the loading conditions. From the above analysis, it can be concluded that the 30Ti_3AlC_2/ZA27 composite exhibits the best mechanical properties.

3 Conclusions

1) A weak reaction occurs at the interface between Ti_3AlC_2 and ZA27 alloy during sintering process of Ti_3AlC_2/ZA27 composite at a temperature of 870 °C, which leads to a good interface bonding between the reinforcement and the matrix. The reaction can be explained by XRD analysis as follow

$$Ti_3AlC_2 \xrightarrow{ZA27} Al_{0.64}Ti_{0.36}+TiC+Al$$

2) Ti_3AlC_2/ZA27 composite with 30 vol% Ti_3AlC_2 reinforcement possesses the best mechanical properties among the four testing materials. And the tensile strength, bending strength and Vickers hardness of the composite are 310 MPa, 528 MPa and 1236 MPa, respectively.

3) The superior mechanical properties for the Ti_3AlC_2/ZA27 composite achieved by pressureless sintering are mainly attributed to a good interfacial bonding, caused by the weak reaction, and dispersion strengthening of nano-sized Ti_3AlC_2 particle. Meanwhile, a fine grain size gotten by planetary ball mixing and uniformly distributed reinforcements are also beneficial to the mechanical properties of the Ti_3AlC_2/ZA27 composites.

References

1 Sastry S, Krishna M, Uchil J. *Journal of Alloys and Compounds*[J], 2011, 314(1-2): 268
2 El-khair M T A, Lotfy A, Daoud A *et al*. *Materials Science and Engineering A*[J], 2011, 528(6): 2353
3 Yu S, Li W, He Z. *Journal of Alloys and Compounds*[J], 2007, 431(1-2): L8
4 Sharma S C, Girish B M, Satish B M *et al*. *Journal of Materials Engineering and Performance*[J], 1998, 7(1): 93
5 Modi O P, Prasad B K, Jha A K. *Wear*[J], 2006, 260(7-8): 895
6 Girish B M, Prakash K R, Satish B M *et al*. *Materials Science and Engineering A*[J], 2011, 530: 382
7 Patnaik A, Mamatha T G, Biswas S *et al*. *Materials & Design*[J], 2012, 36: 511
8 Huang Z Y, Bonneville J, Zhai H X *et al*. *Journal of Alloys and Compounds*[J], 2014, 602: 53
9 Lu J R, Zhou Y, Zheng Y *et al*. *Advances in Applied Ceramics*[J], 2015, 114(1): 39
10 Guo H P, Zhang J, Li F Z *et al*. *Journal of the European Ceramic Society*[J], 2008, 28(10): 2099
11 Gu W L, Yan C K, Zhou Y C. *Scripta Materialia*[J], 2003, 49(11): 1075
12 Zhang J, Wang J Y, Zhou Y C. *Acta Materialia*[J], 2007, 55(13): 4381
13 Shi X L, Wang M, Zhai W Z *et al*. *Materials & Design*[J], 2013, 45: 179
14 Shi X L, Zhai W Z, Xu Z S *et al*. *Materials & Design*[J], 2014, 55: 93
15 Amini S, Barsoum M W. *Materials Science and Engineering A*[J], 2010, 527(16-17): 3707
16 Wang X H, Zhou Y C. *Acta Materialia*[J], 2002, 50(12): 3143
17 Wang Y, Xie N S, Li C Y *et al*. *Foundry Technology*[J], 2010, 31(5): 656 (in Chinese)
18 El-Raghy T, Barsoum M W, Zavaliangos A *et al*. *Journal of the American Ceramic Society*[J], 1999, 82(10): 2855
19 Sun Z M. *International Materials Reviews*[J], 2011, 56(3): 143
20 Ai M X, Zhai H X, Zhou Y *et al*. *Journal of the American Ceramic Society*[J], 2006, 89(3): 1114
21 Li H Y, Zhou Y, Chen C *et al*. *Advances in Applied Ceramics*[J], 2015, 114: 315
22 Pang W K, Low I M, Sun Z M. *Journal of the American Ceramic Society*[J], 2010, 93(9): 2871
23 Zhang J, Wang J Y, Zhou Y C. *Acta Materialia*[J], 2007, 55(13): 4381
24 Girish B M, Prakash K R, Satish B M *et al*. *Materials & Design*[J],

2011, 32: 1050
25 Barsoum M W, Radovic M. *Annual Review of Materials Research*[J], 2011, 41: 195
26 Peng L M. *Scripta Materialia*[J], 2007, 56(9): 729
27 Mishra S K, Biswas S, Satapathy A. *Materials & Design*[J], 2014, 55: 958

Ti_3AlC_2 颗粒含量对 Ti_3AlC_2/ZA27 复合材料性能的影响

李海燕，周　洋，崔　傲，李世波，黄振莺，翟洪祥
(北京交通大学，北京 100044)

摘　要：通过无压烧结技术和机械合金化技术，在烧结温度为 870 ℃，保温时间为 2.5 h 的工艺条件下，制备了 4 种含有不同体积分数的 Ti_3AlC_2 颗粒的 Ti_3AlC_2/ZA27 复合材料。研究了 Ti_3AlC_2 颗粒含量对 Ti_3AlC_2/ZA27 复合材料的硬度、密度，拉伸强度和弯曲强度的影响。结果表明界面处的微弱化学反应有助于提高复合材料的界面结合能力，进而提高 Ti_3AlC_2/ZA27 复合材料的机械性能。此外，随着 Ti_3AlC_2 颗粒含量增多，Ti_3AlC_2/ZA27 复合材料的硬度和力学强度都随之增大，这主要归因于纳米尺度的 Ti_3AlC_2 颗粒的弥散增强结果。然而，随着 Ti_3AlC_2 颗粒增加到 40 vol%，由于孔隙的增多，Ti_3AlC_2/ZA27 复合材料的硬度和力学强度又出现下降。对比制得的 4 种 Ti_3AlC_2/ZA27 复合材料，30Ti_3AlC_2/ZA27 复合材料具有最大的抗拉强度、抗弯曲强度以及维氏硬度，分别为 310，528 和 1236 MPa。这些优异的性能除了归因于良好的界面结合，还归因于 Ti_3AlC_2 颗粒的细晶强化和弥散强化作用。

关键词：Ti_3AlC_2/ZA27 复合材料；界面；机械性能

作者简介：李海燕，女，1989 年生，博士生，北京交通大学机械与电子控制工程学院，北京 100044，电话：010-51685554，E-mail: 13116356@bjtu.edu.cn